NASA TECHNICAL NOTE

NASA TN D-2881

NASA TN D-2881

A MIXING MODEL FOR ROCKET ENGINE COMBUSTION

by Martin Hersch

Lewis Research Center

Cleveland, Ohio

NATIONAL AERONAUTICS AND SPACE ADMINISTRATION • WASHINGTON, D. C. • JUNE 1965

NASA TN D-2881

A MIXING MODEL FOR ROCKET ENGINE COMBUSTION

By Martin Hersch

Lewis Research Center
Cleveland, Ohio

NATIONAL AERONAUTICS AND SPACE ADMINISTRATION

For sale by the Clearinghouse for Federal Scientific and Technical Information
Springfield, Virginia 22151 – Price $1.00

A MIXING MODEL FOR ROCKET ENGINE COMBUSTION

by Martin Hersch

Lewis Research Center

SUMMARY

2660 l

A model for predicting rocket combustion performance is presented which is based on the assumption that performance is limited only by gas-phase turbulent diffusion, or mixing, of oxidant and fuel vapors. The model shows how mixture ratio, chamber length, injector-hole spacing, and turbulence intensity affect performance. The results of detailed calculations performed on an IBM 7090 computer for a number of propellant systems are presented.

Author

INTRODUCTION

Many physical processes occur simultaneously in a rocket combustor. In order to understand the importance of the various processes, such as vaporization, gas-phase mixing, or chemical reaction, each one is considered separately so that their effects on combustor performance may be determined and compared. The vaporization process in rocket combustion is well understood, and an exhaustive analysis of it is presented in reference 1. Chemical reaction rates are usually considered to be very rapid and therefore not a limiting factor in controlling the rocket combustion process. A treatment of the relative importance of chemical reaction rates in rocket combustion is presented in reference 2. The mixing process, though less well understood, may possibly be, under certain conditions, a rate limiting step in the combustion process. Mixing in rocket combustion is considered in references 3 to 12.

In essence, the model developed herein combines the highly generalized results of reference 3 with a technique similar to that suggested in reference 1 (p. 50). In reference 1 it is suggested that the effect of mixing on performance may be determined by calculating the performance of many small areas in a combustor cross section and averaging the results. The results of reference 3 show how propellant concentration varies radially across the combustor as a function of chamber length, injector-hole spacing, and intensity of turbulence, but do not indicate what effect such variations might have on combustor performance.

The objective of this study is to translate the generalized concentration profiles of reference 3 into combustor performance values. A model based on that of reference 3 is presented which enables mixing-limited performance to be calculated for particular propellant systems as a function of chamber length, turbulence intensity, injector-hole spacing, and operating propellant mixture ratio. Results of detailed digital computor calculations using this model are presented for eight propellant systems: oxygen with hydrogen, ammonia, hydrazine, and JP-4; fluorine with hydrogen, ammonia, and hydrazine; and nitrogen tetroxide with hydrazine.

SYMBOLS

A	area, sq ft
C^*	characteristic exhaust velocity, ft/sec
$\mathscr{C}$	radial concentration of oxidizer or fuel, mass per unit volume
c	proportionality factor (eq. (6))
F	fuel mass flow, lb/sec
$\mathscr{F}$	fractional fuel composition, m_F/m_t
K, k	proportionality constants (eq. (2))
L	chamber length, in.
M	molecular weight
m	mass flow
n	number of annular equal-area concentric rings
O	oxidant mass flow, lb/sec
P	pressure, lb/sq in.
R	universal gas constant
r	radial distance from axis of source, in.
r'	$r/(S/2)$
S	injector-hole spacing, in.
T	intensity of turbulence, fluctuating or root mean square velocity/mean free stream velocity, percent

V velocity

α mixing parameter, $T\frac{L}{S}$

ρ gas density, lb/cu ft

ψ mixing efficiency or ripple factor, $(O/F)_{min}/(O/F)_{max}$, percent

Subscripts:

F fuel

i annular ring i

max maximum

min minimum

O oxidant

t total or metered value

THEORY AND MODEL FOR CALCULATING PERFORMANCE

The diffusion of a rocket propellant component injected from a grid of point sources into an infinite flowing stream of the other propellant component is treated in reference 3. The extent of mixing or the mixing efficiency is expressed as a "ripple factor," which is the ratio of minimum to maximum radial concentration of a propellant component in a plane parallel to the injector face:

$$\psi = \mathscr{C}_{min}/\mathscr{C}_{max}$$

The value of ψ is unity for complete mixing and zero for no mixing. The mixing parameter is the product of intensity of turbulence and the ratio of chamber length to injector hole spacing:

$$\alpha = T\frac{L}{S}$$

The model of reference 3 is strictly applicable only for dilute mixtures of the diffusing material. The mixtures encountered in a rocket combustor may, however, vary from extremely fuel rich to extremely oxidant rich. To facilitate the calculations for rocket combustors, the ripple factor is redefined so that it represents the ratio of minimum to maximum oxidant-fuel mass ratios occurring in the plane parallel to the injector face:

$$\psi = (O/F)_{min} \Big/ (O/F)_{max} \tag{1}$$

The oxidant-fuel ratio rather than the concentration ratio of one component will be assumed to vary radially in a gaussian manner, as described in reference 3.

As in reference 3, the injector will be considered to consist of an infinite grid of sources of one propellant injected into a flowing stream of the other propellant. If it is assumed that the oxidant diffuses from the sources, then in any downstream plane parallel to the injector face the O/F will have maximum points on the axes of the sources and minimum points between these axes. Because of the symmetry of the system, only one-half of an O/F variation cycle need be considered. The O/F distribution is assumed to vary in a gaussian manner from the maximum to the minimum points:

$$\frac{O}{F} = Ke^{-kr^2} \tag{2}$$

The radial distance from the axis of the source to the point of minimum concentration is assumed to be one-half of the grid source spacing S. A nondimensional radius may be defined as

$$r' = \frac{r}{S/2} \tag{3}$$

S/2 being the radial distance from maximum to minimum O/F. The value of r' then becomes 0 on the axis of the source, or point of maximum O/F, and unity at the point of minimum O/F. It follows that the proportionality factors K and k are given by $K = (O/F)_{max}$ and $\psi = e^{-k}$. The intermediate O/F at any radial position r_i may be written

$$(O/F)_i = (O/F)_{max}\psi^{r_i'^2} \tag{4a}$$

In an analogous fashion the fuel could be considered to diffuse from the sources surrounded by oxidant, and the result is

$$(O/F)_i = (O/F)_{min}\psi^{-r_i'^2} \tag{4b}$$

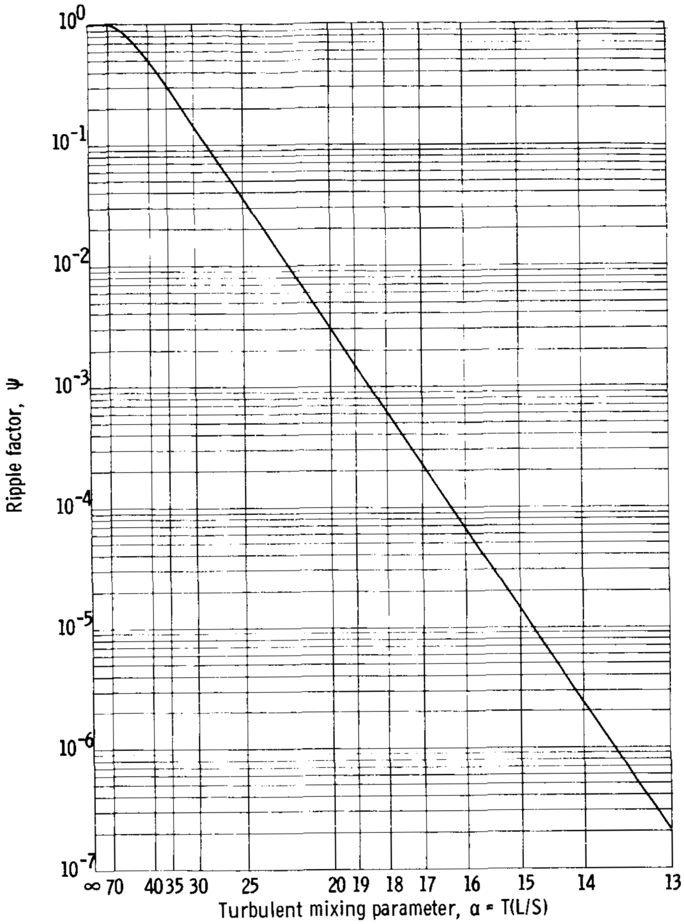

Figure 1. - Ripple factor as function of turbulent mixing parameter. (Turbulence T is in percent.)

As shown in reference 3, the mixing efficiency, or ripple factor, ψ may be related to combustor length L, intensity of turbulence T, and injector-hole spacing S. The results, based on equation (7) of reference 3, are shown in figure 1 as a function of the turbulent mixing parameter $\alpha = T(L/S)$.

Since it is sufficient to consider only one-half of a cycle of O/F variation to characterize an entire combustor, the axis of one of the sources can be considered to be the center or axis of a combustor and the point of minimum O/F to be the wall of the combustor. This single-source combustor is now considered to be composed of a large number of equal-area annular rings, all at equal pressure and having equal gas velocities. This approach is similar to that of reference 6. The average O/F of each ring now depends upon its mean radius according to equation (4a).

The mass flow through each of the equal-area rings can now be computed from the continuity equation:

$$m = \rho AV = \frac{PM}{RT} AV \tag{5}$$

The thermodynamic equilibrium molecular weight and the temperature in each ring are functions of the ring composition, as computed from equation (4a). When the composition is known, the temperature and the molecular weight can be obtained by using the method of reference 13. Since the rings are of equal area and it is assumed that there are no pressure or velocity gradients across the combustor, the mass flow through the rings may be written

$$m_i = c \frac{M_i}{T_i} \tag{6}$$

Inasmuch as only the ratios of the mass flow in each ring to total mass flow in the system enter into the subsequent equations, the proportionality factor need not be computed and, therefore, does not appear in the equations that follow.

Since vaporization is assumed to be completed before the start of mixing, the initial state of the propellants is gaseous. The overall performance, expressed as characteristic exhaust velocity C^* may now be computed from the relative mass flows and equilibrium C^* values according to the composition (also from ref. 13) in each ring:

$$C^* = \frac{1}{m_t} \sum_{i=1}^{n} m_i C_i^* \tag{7a}$$

where

$$m_t = \sum_{i=1}^{n} m_i \tag{7b}$$

It is assumed that there is no mass or heat transfer between rings, that the gases in each ring attain chemical thermodynamic equilibrium conditions, and that the gases of each ring, when passing through the exhaust nozzle, adjust to the area needed for sonic, that is, choked flow.

Since it is necessary in this model to handle an extremely wide range of values for the mixture ratio, the calculations are facilitated by expressing mixture composition in terms of fractional fuel content. Thus the composition in each ring is then written as

$$\mathscr{F}_i = \frac{1}{(O/F)_{max} \psi^{r_i^2} + 1} \tag{8}$$

The total, or metered, fuel fraction and O/F can be computed from

$$\mathscr{F}_t = \frac{1}{m_t} \sum_{i=1}^{n} (\mathscr{F}_i m_i) \tag{9}$$

$$(O/F)_t = (1/\mathscr{F}_t) - 1 \tag{10}$$

The method of reference 13 can also be used to determine the C^* corresponding to the metered mixture ratio. This then, is the C^* that the combustor would attain if all reactants were perfectly mixed and combustion was completed. The ratio of the C^* calculated from equation (7a) to this value is therefore the C^* efficiency of a combustor having imperfectly mixed propellants.

The input data for the computer program consisted of tables of equilibrium temperature, molecular weight, and C^* as functions of initial mixture composition expressed as fuel fractions. These data were obtained from the program described in reference 13. The other input data were values of ripple factor, number of rings, and $(O/F)_{max}$. The metered O/F is, unfortunately, unknown beforehand when this model is used. Therefore the values of $(O/F)_{max}$ were arbitrarily chosen. A few preliminary runs were made to determine appropriate values of $(O/F)_{max}$ needed to generate desirable metered O/F values at a given ripple factor.

The input data, obtained by using the method of reference 13 for characteristic exhaust velocities, temperatures, and molecular weights as functions of the fuel fraction composition of gaseous reactants, are given in table I. A three-point logarithmic Lagrangian interpolation technique was used to evaluate properties between tabulated compositions.

The number n of annular concentric equal-area rings was 100. A few calculations performed with a greater number indicated 100 to be sufficient. The radius r_i at which composition and properties were determined was the arithmetic mean radius of each ring; it was assumed that for a large number of rings the composition could be considered uniform in any one ring.

The ripple factor may be determined from the following equation:

$$\log \psi = 0.497 - \frac{1210}{\alpha^2} \tag{11}$$

where α is evaluated by using turbulence in percent. This equation may be applied to the linear portion of the curve shown in figure 1 if the curve is assumed to be linear for all values of α less than about 37. This curve indicates that mixing is completed for an α of about 70.

The propellants, if complete vaporization is assumed, will produce some characteristic exhaust velocities even though there should be no mixing of oxidant with fuel, and therefore no burning. For this situation the values of α and ψ become zero, and equations (4) and (8) may become, in this limit, indeterminant. By applying equation (7a) with $n = 2$ for the two regions of pure oxidant and pure fuel, it can be shown that the C^*

for the case of no mixing is given by

$$C^* = \frac{1}{(O/F)_t + 1}\left[C^*_F + (O/F)_t C^*_O\right] \tag{12}$$

It is also possible, by using the continuity equation, to calculate the flow areas for oxidant and fuel for the case of no mixing. It can be shown that for the model, as used herein, the sources are not true points, but possess finite area. The ratio of oxidant to fuel injection area is given by

$$A_O/A_F = (O/F)_t(\rho_F/\rho_O) \tag{13}$$

For very dilute mixtures, that is, low O/F values such as those considered in reference 3, the source reduces to a point.

RESULTS AND DISCUSSION

Calculated Effects of Incomplete Mixing

Detailed calculations to determine the effects of incomplete propellant mixing on combustor performance were made for the following eight propellant systems:

(1) Oxygen with

- (a) Hydrogen
- (b) Ammonia
- (c) Hydrazine
- (d) JP-4 fuel

(2) Fluorine with

- (a) Hydrogen
- (b) Ammonia
- (c) Hydrazine

(3) Nitrogen tetroxide with hydrazine

Results of the calculations are shown in figure 2. Values of C^* and C^* efficiency are presented as functions of the calculated metered O/F with α as a parameter. The uppermost performance curve in each part of figure 2 is a plot of the theoretical C^* values corresponding to perfect mixing ($\alpha \geq 70$) and equilibrium conditions as obtained

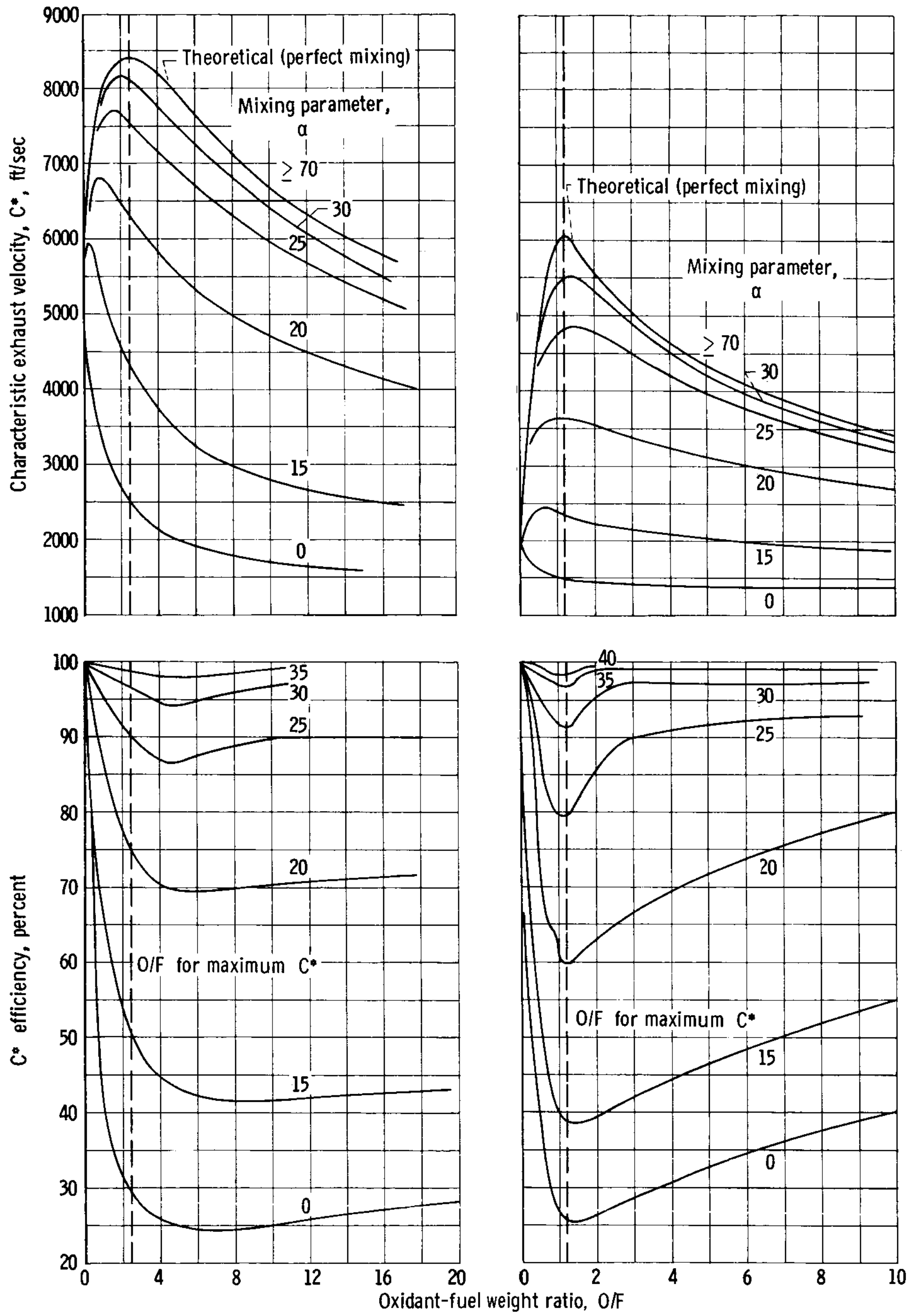

(a) Oxygen-hydrogen system. (b) Oxygen-ammonia system.

Figure 2. - Effect of incomplete mixing on rocket combustor performance.

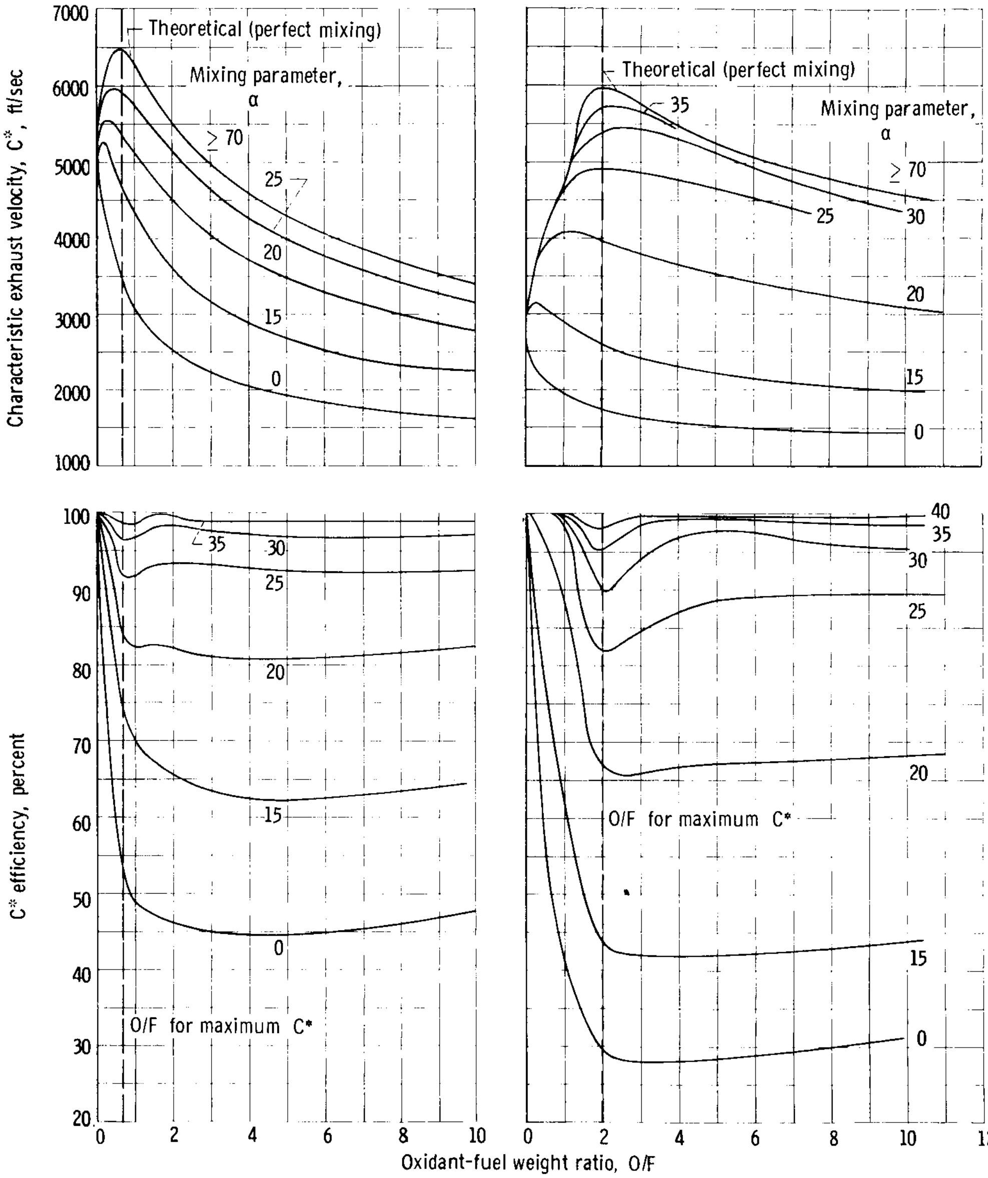

(c) Oxygen-hydrazine system.

(d) Oxygen - JP-4 system.

Figure 2. - Continued.

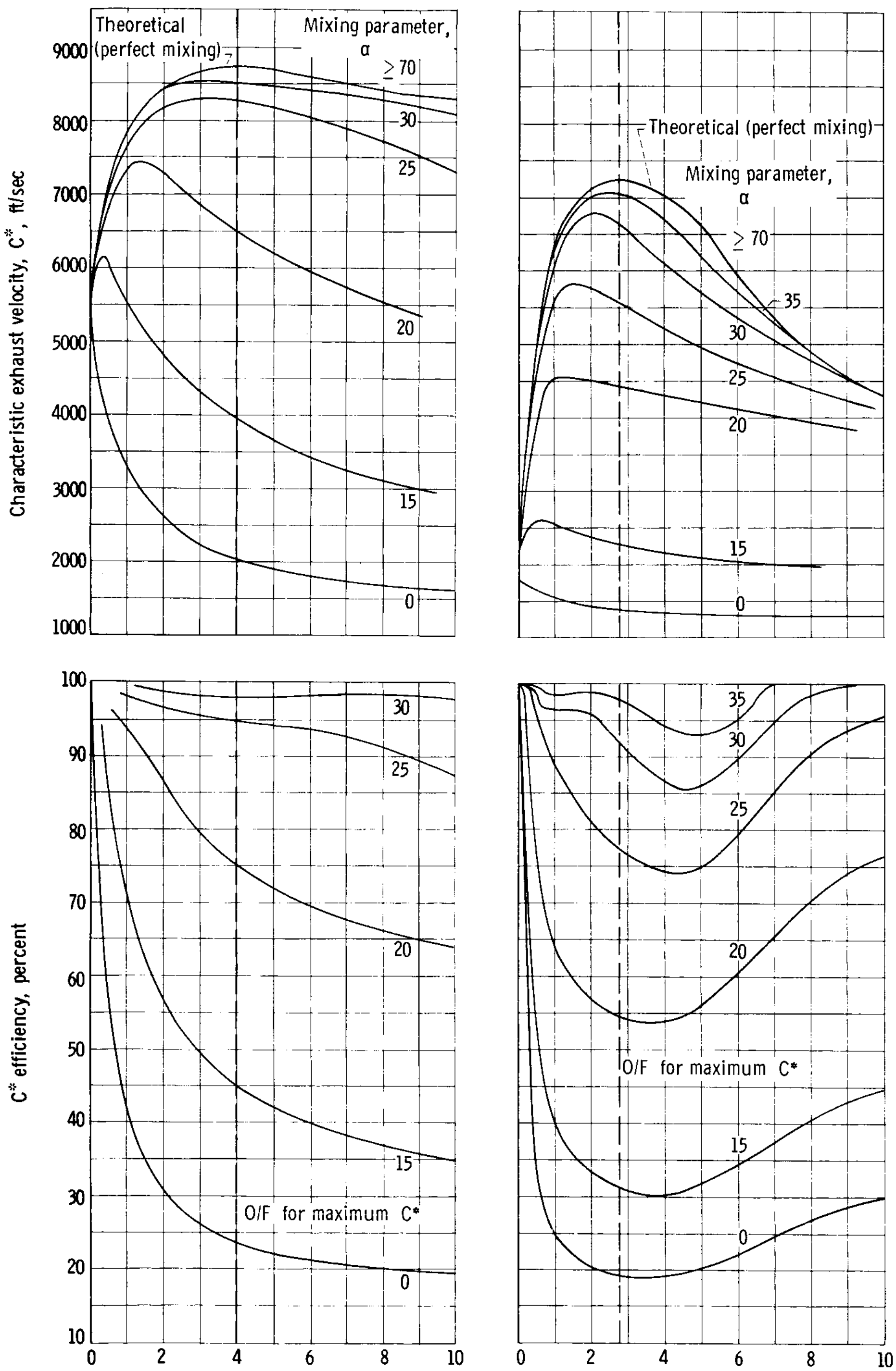

(e) Fluorine-hydrogen system.

(f) Fluorine-ammonia system.

Figure 2. - Continued.

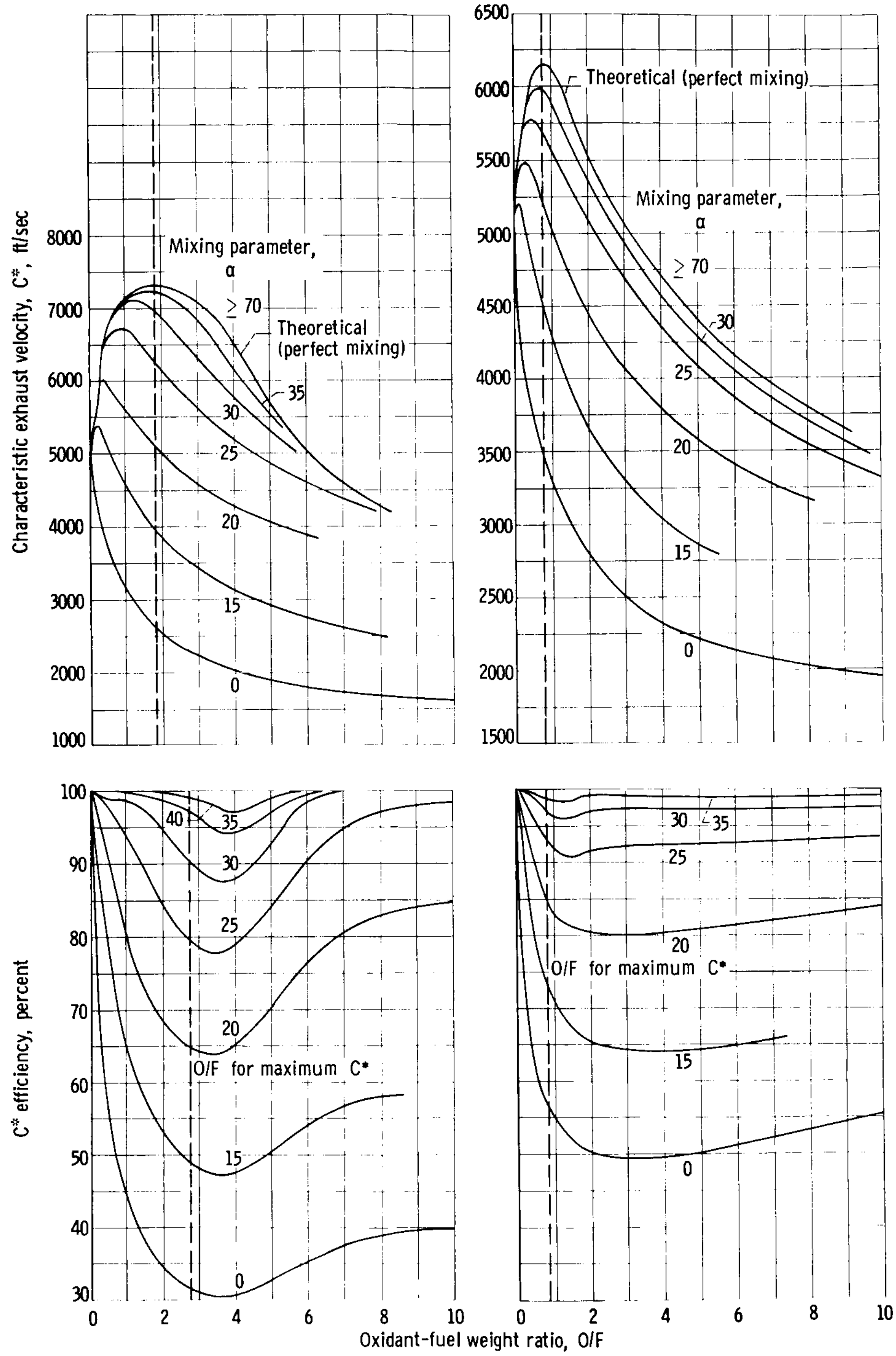

(g) Fluorine-hydrazine system.

(h) Nitrogen tetroxide-hydrazine system.

Figure 2. - Concluded.

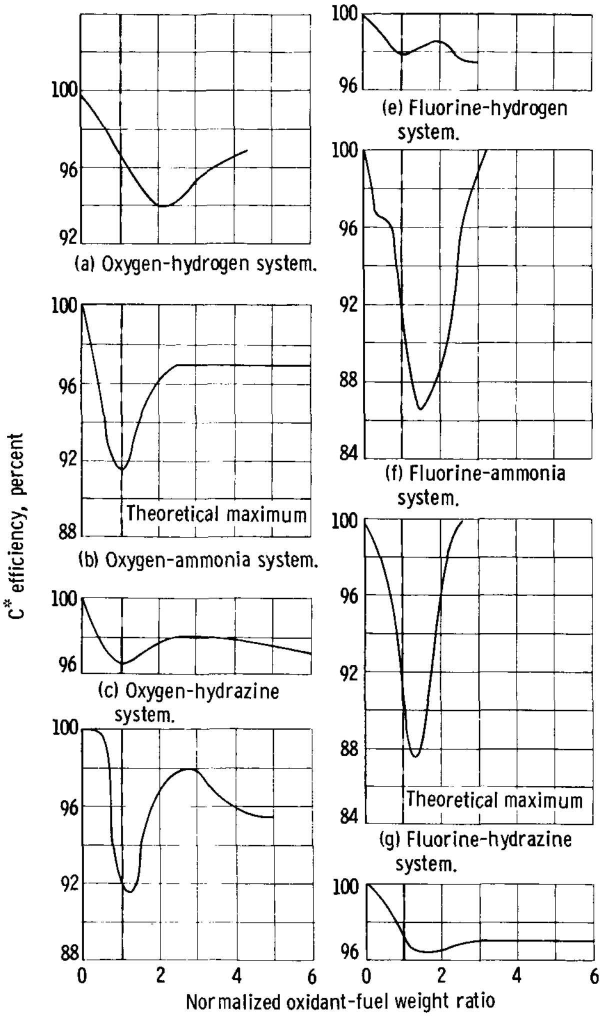

(a) Oxygen-hydrogen system.
(b) Oxygen-ammonia system.
(c) Oxygen-hydrazine system.
(d) Oxygen - JP-4 system.
(e) Fluorine-hydrogen system.
(f) Fluorine-ammonia system.
(g) Fluorine-hydrazine system.
(h) Nitrogen tetroxide-hydrazine system.

Figure 3. - Efficiency as function of oxidant-fuel weight ratio divided by that for maximum theoretical characteristic exhaust velocity. Mixing parameter, 30.

from reference 4. The lowest curves in each part of figure 2 indicate the C* and C* efficiency that would be attained if both propellants were completely vaporized and flowing through the combustor with no mixing as calculated from equation 12. All calculations were made at a chamber pressure of 300 pounds per square inch. Only the O/F regions likely to be of interest to a combustor designer, from 0 to 10, are shown. The model can, however, be used to calculate performance at any $O/\bar{F}$, by simply inserting appropriate values of $(O/\bar{F})_{max}$ into equation (8).

The C* curves for a mixing efficiency of zero (fig. 2) indicate that the performance is a smooth function of O/F and is, for no mixing, always bounded by the C* values of pure fuel and pure oxidant. As mixing increases, the curves progressively assume the shape and values of the theoretical curve.

The performance efficiency is of course 100 percent for either pure fuel or pure oxidant. It is seen that in most cases the C* performance tends to be a maximum and the C* efficiency a minimum near the O/F corresponding to the maximum or peak C* (indicated by the vertical dotted lines for the perfectly mixed propellants). The sharpness of these maximum and minimum points are seen to depend on the particular propellant system in question and the mixing efficiency. The maximum C* performance values appear almost always to be fuel rich with respect to the O/F for peak theoretical C*. In contrast, the minimum C* efficiencies appear almost always to occur at mixtures that are oxidant rich with respect to the O/F of peak theoretical C*.

The curves for the oxygen-hydrogen, oxygen-hydrazine, oxygen - JP-4, and nitrogen tetroxide - hydrazine systems (figs. 2(a), (c), (d), and (h), respectively) show that the C* efficiency is extremely sensitive to mixture ratio in the very fuel rich region, dropping off very rapidly with increasing metered O/F, and then leveling off or in-

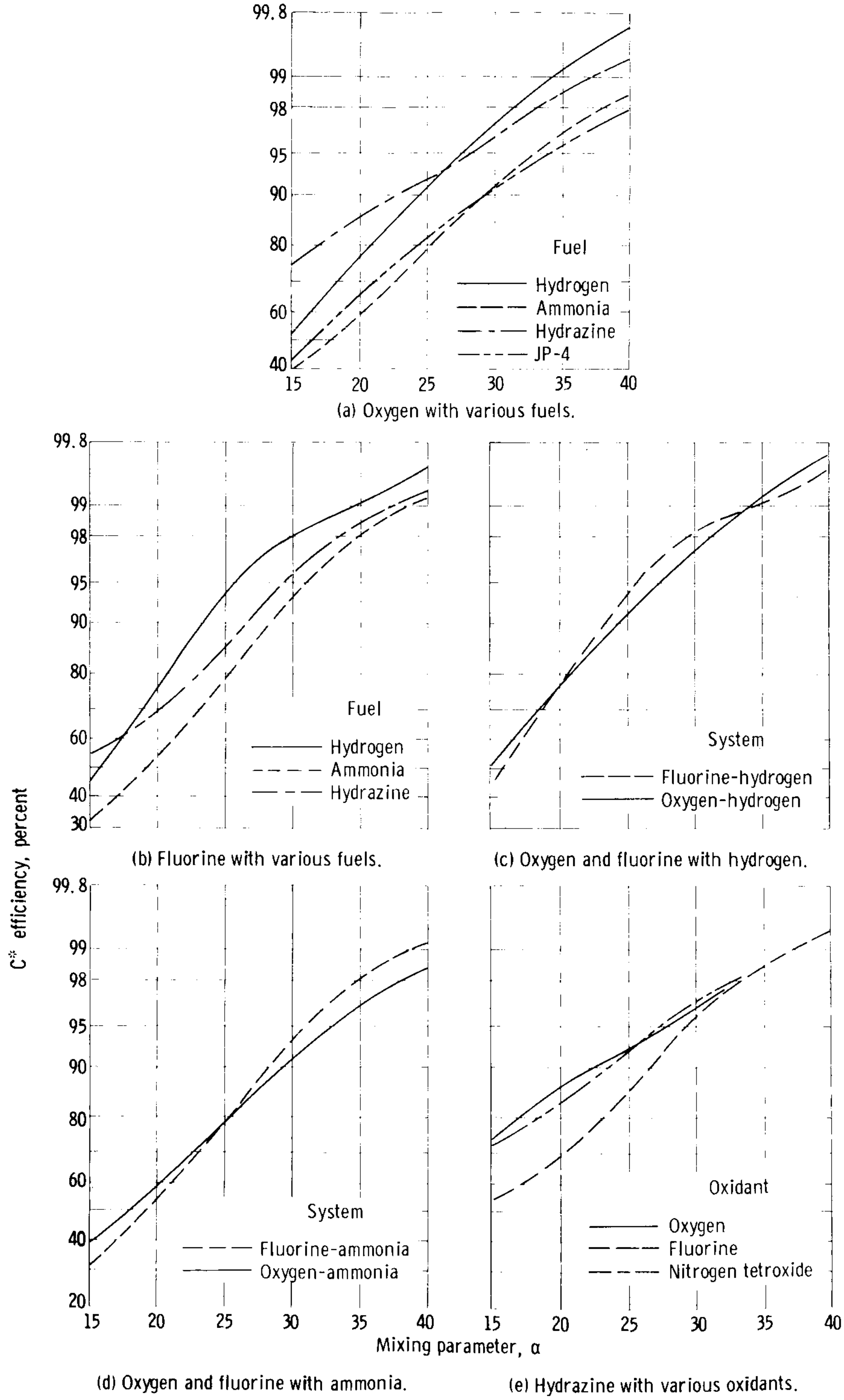

Figure 4. - Characteristic exhaust velocity efficiency as function of mixing parameter at oxidant-fuel weight ratio for maximum theoretical characteristic exhaust velocity.

creasing slightly with O/F. The efficiency for the fluorine-hydrogen system decreases more gradually with O/F in the region shown.

To compare more readily the effect of mixing on efficiency for various systems, all the systems are shown in figure 3, where efficiency is plotted as a function of normalized O/F for an α of 30. The normalized O/F is the ratio of the metered O/F to the O/F corresponding to peak theoretical C^*.

The relative importance of mixing for the various propellant systems is also shown in figure 4, where C^* efficiency is plotted as a function of the mixing parameter for the various systems. All the curves are for a mixture ratio corresponding to peak theoretical C^*, that is, a normalized O/F of 1. Oxygen with various fuels is shown in figure 4(a), and fluorine with various fuels in figure 4(b). Figure 4(c) compares the hydrogen-fluorine and hydrogen-oxygen systems, figure 4(d) compares the ammonia-oxygen and ammonia-fluorine systems, and figure 4(e) compares the performance of hydrazine when burned with oxygen, fluorine, and nitrogen tetroxide.

In figure 4(a), it is seen that at low values of α (poor mixing conditions) best performance with oxygen is obtained when it is burned with hydrazine. As mixing is improved, however, the best performance is obtained when the oxygen is burned with hydrogen. With fluorine as the oxidizer (fig. 4(b)) the best performance is obtained with hydrogen as a fuel.

With hydrogen as a fuel (fig. 4(c)) little change is obtained in going from fluorine to oxygen. Such is also the case in figure 4(d), where ammonia is shown as the fuel. With hydrazine as a fuel, however, figure 4(e) shows that, for low values of α, performance is markedly lower with fluorine as an oxidizer than with either nitrogen tetroxide or oxygen, both of which result in nearly the same performance. With improved mixing the performance with fluorine becomes equal to that obtained with the other oxidizers.

All calculations were made with the oxidant in the center diffusing into the fuel. The results were unchanged when the fuel was in the center.

An example of the variations in radial reactant composition for different degrees of mixing is shown in figure 5. The case shown is for oxygen-hydrogen at a metered O/F of 3 with oxygen in the center. For perfect mixing the composition would be uniform across the combustor, which for the case shown is an O/F of 3. For no mixing the composition would be pure oxygen up to a nondimensional radius of about 0.4. The family of curves indicates then that the radial composition profiles are a function of mixing efficiency. It is seen in figure 5 that with even very slight mixing ($\alpha = 5.8$, $\psi = 3.13\times10^{-35}$) an appreciably wide mixing zone exists at the interface of pure propellants.

One interesting result of this analysis is that in all cases near-perfect performance appears to be attained with mixing parameter values of 35 to 40. This is rather significant, because an α of 35 to 40 corresponds to a ripple factor of 1/3 to 1/2, that is, a

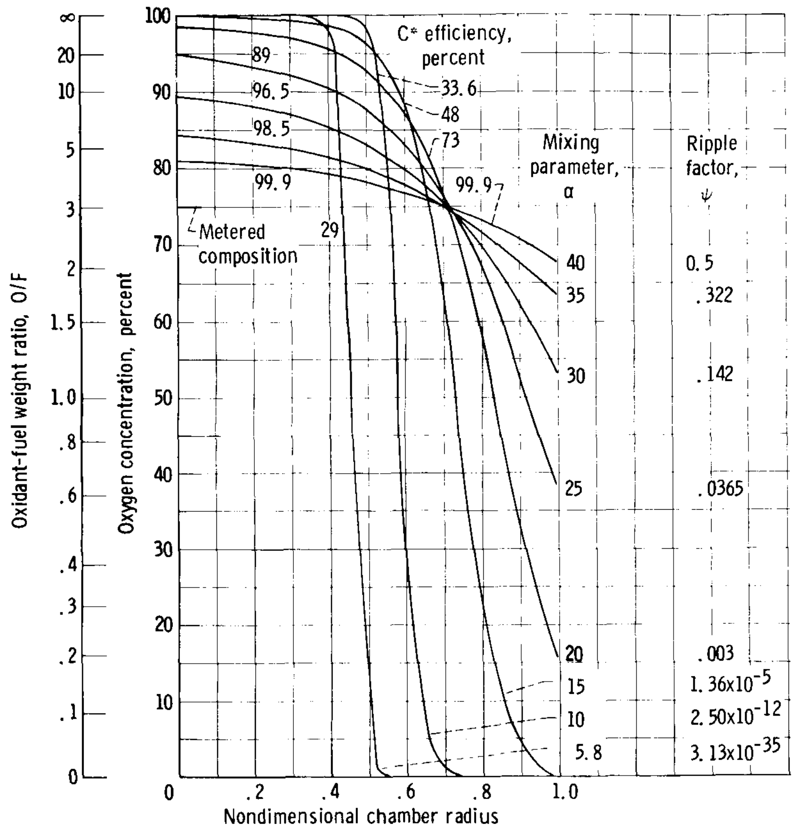

Figure 5. - Radial reactant composition across mixing zone for various values of mixing parameter. Oxygen in center.

mixing efficiency of about 30 to 50 percent. This result could be of importance in situations where it is desired to have O/F variations across the combustor. For example, in certain cases, it may be necessary to have the propellant mixture be fuel rich near the wall for cooling purposes, but yet not have this result in a significant performance loss. The results of this study, as illustrated in figure 5, indicate the possibility of having such O/F gradients with little performance loss.

Because of the many simplifying assumptions made in reducing the complex turbulent diffusion theory to the working model in reference 3 and the further assumptions of this study, it is not intended that the results herein be taken to have any great degree of rigor. The results, however, do give some quantitative effects of mixing on rocket combustion that have not been heretofore available.

For example, the results of this study indicate that, in general, the oxidant-fuel mixture ratio for high performance may be near that for lowest C* efficiency. The results also indicate which propellant systems are most likely to be sensitive to O/F changes and in what O/F ranges these changes are likely to be most important.

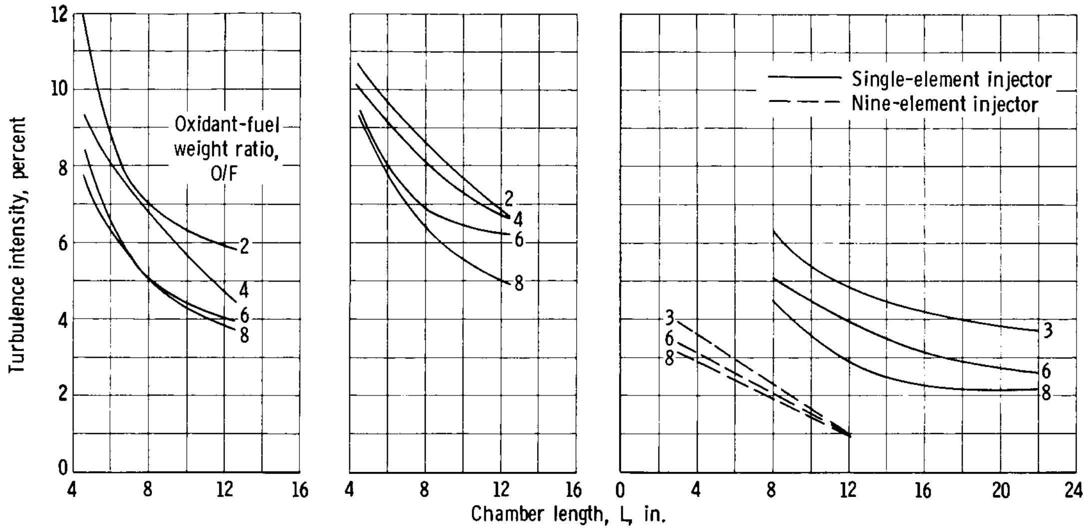

(a) Liquid oxygen in center; data from reference 4.

(b) Liquid oxygen in annulus; data from reference 4.

(c) Liquid oxygen in center; data from reference 9.

Figure 6. - Intensity of turbulence calculated by using experimental data and mixing model.

Comparison With Experimental Data

An experimental study of rocket combustor performance is presented in reference 9. In this study performance was evaluated as a function of O/F for a liquid-oxygen - gaseous-hydrogen combustor with various injectors. The injectors were designed so that the oxygen atomization and mixing could be varied. The O/F was varied from about 2 to 10. With injectors having poor atomization characteristics C* efficiency increased with increasing O/F, and with injectors having poor mixing characteristics C* efficiency decreased with increasing O/F. The predicted performance trends with O/F for the oxygen-hydrogen system, as shown in figure 2(a), therefore agree with experimental data.

The difficulty in applying the results of this model to predict the performance of a combustor is the availability of the turbulence intensity value so that the mixing parameter α may be evaluated. There is little information about turbulence values in rocket combustors. Qualitative photographic studies (refs. 10 and 11) have indicated that turbulence intensity is high near the injector face and decreases with chamber length. Quantitatively, it varied (ref. 12) from as high as 10 percent at the injector to about 2 percent 8 inches downstream. Turbulence values for the oxygen-hydrogen system calculated by using the experimental performance data of references 4 and 9 and corresponding values of the mixing parameter are presented in figure 6.

These turbulence values were calculated from the value of α corresponding to the experimental performance and O/F by using the curves of figure 2(a). Then, since the chamber length and injector-hole spacing were known, the turbulence intensity was calculated. For computing α from the data of reference 4, the effective mixing length L was assumed to include the chamber length plus the 3-inch convergence nozzle length. For the single-element injectors the effective hole spacing S was considered to be 2 inches, the chambers being 2 inches in diameter. The hole spacing for the nine-element injector of reference 9 was considered to be 3/8 inch. The injectors were of the concentric tube type; that is, one propellant was injected from a central tube surrounded by an annular injector for the other propellant. The liquid oxygen was poorly atomized when injected from the tube and well atomized when injected from the annulus. In all cases turbulence decreases with increasing chamber length and increasing O/F. It is highest for the single-element injectors when the oxygen is centrally injected, somewhat lower when the hydrogen is centrally injected, and significantly lower when the number of elements is increased from one to nine. The effective hole spacing for the nine-element injector may have been somewhat greater than the actual spacing of 3/8 inch because the holes were concentrated in the central area of the injector face. Assuming a more uniform spacing would have raised somewhat the turbulence value shown in figure 5 for the nine-element curves. It is intended that these curves give some idea of approximate turbulence values that may be anticipated in a combustor so that this model may be useful in predicting performance.

CONCLUDING REMARKS

An attempt was made to determine the effect of incomplete propellant mixing on rocket combustor performance. Because of the complexity of turbulent diffusion theory, a highly simplified model was necessarily used. It is not intended that the results presented herein be taken to have a great deal of precision, but rather that they be used as a helpful aid in designing rocket combustors, in furthering the understanding of rocket combustion, and in complementing the vaporization-limited models for rocket combustion. The model may also be helpful in interpreting experimental data.

It should not be inferred that the model presented herein can be applied only to the idealized injection scheme of reference 3 or to concentric injector schemes. This model can be applied to any scheme of injection that results in mixture variations across the injector face. In applying the model, each element of the injector, whether concentric, impinging-jet, like-on-like, or of any other type, may be considered as constituting a source in reference to this model. The effective source spacing S would then be taken to be the distance between injector elements, even though both propellants are injected from each element.

SUMMARY OF RESULTS

A model for predicting rocket combustor performance has been developed based on the assumption that performance is limited by gaseous turbulent diffusion. Detailed calculations were made for chamber length, injector-hole spacing, and intensity of turbulence for a number of propellant systems. The resulting curves give performance as a function of the mixture ratio and a mixing parameter. The following are the most salient conclusions of this study:

1. The effect of mixing on rocket combustor performance is a function of the propellant system, the mixture ratio, and a mixing parameter which is the product of turbulence intensity and the ratio of combustor length to injector-hole spacing.

2. For all the propellant systems considered the effect of mixture ratio appears to be most pronounced in the region corresponding to that of the maximum theoretical characteristic exhaust velocity C^* of the perfectly mixed propellants. The maximum C^* performance was fuel rich with respect to the C^* for peak performance. The minimum C^* efficiency was always oxidant rich with respect to the oxidant-fuel ratio needed for peak theoretical C^*.

3. Complete mixing need not be a necessary condition to attain high engine performance. In all cases considered, high-performance efficiency is predicted with as great as a 2 to 1 or even 3 to 1 variation in mixture ratio across the combustor.

Lewis Research Center,
National Aeronautics and Space Administration,
Cleveland, Ohio, March 19, 1965.

REFERENCES

1. Priem, Richard J.; and Heidmann, Marcus F.: Propellant Vaporization as a Design Criterion for Rocket-Engine Combustion Chambers. NASA TR R-67, 1960.

2. Bittker, David A.; and Brokaw, Richard S.: Estimate of Chemical Space Heating Rates in Gas-Phase Combustion With Application to Rocket Propellants. ARS J., vol. 30, no. 2, Feb. 1960, pp. 179-185.

3. Bittker, David A.: An Analytical Study of Turbulent and Molecular Mixing in Rocket Combustion. NACA TN 4321, 1958.

4. Hersch, Martin: Effect of Interchanging Propellants on Rocket Combustor Performance With Coaxial Injection. NASA TN D-2169, 1964.

5. Lewis, J. D.: Some Basic Studies of Liquid Propellant Injection Processes. J. Roy. Aeron. Soc., vol. 68, no. 647, Nov. 1964, pp. 743-750.

6. Bryan, R.: The Sampling of Rocket Combustion Gases. J. Roy. Aeron. Soc., vol. 68, no. 647, Nov. 1964, pp. 759-764.

7. Wrobel, J. R.: Some Effects of Gas Stratification on Choked Nozzle Flows. Paper No. 64-266, AIAA, 1964.

8. Altman, David; and Lorell, Jack: Effect of Local Variations in Low Mixture Ratio on Rocket Performance. ARS J., vol. 22, no. 5, Sept.-Oct. 1952, pp. 252-255.

9. Heidmann, M. F.; and Baker, Louis, Jr.: Combustor Performance With Various Hydrogen-Oxygen Injection Methods in a 200-Pound-Thrust Rocket Engine. NACA RM E58E21, 1958.

10. Altseimer, John H.: Photographic Techniques Applied to Combustion Studies - Two-Dimensional Transparent Thrust Chamber. ARS J., vol. 22, no. 2 Mar.-Apr. 1952, pp. 86-91.

11. Bellman, Donald R.; Humphrey, Jack C.; and Male, Theodore: Photographic Investigation of Combustion in a Two-Dimensional Transparent Rocket Engine. NACA Rept. 1134, 1953.

12. Hersch, Martin: Experimental Method of Measuring Intensity of Turbulence in a Rocket Chamber. ARS J., vol. 31, no. 1, Jan. 1961, pp. 39-45.

13. Zeleznik, Frank J.; and Gordon, Sanford: A General IBM 704 or 7090 Computor Program for Computation of Chemical Equilibrium Compositions, Rocket Performance, and Chapman-Jouguet Detonations. NASA TN D-1454, 1962.

TABLE I. - EQUILIBRIUM MOLECULAR WEIGHT, TEMPERATURE, AND CHARACTERISTIC EXHAUST VELOCITY AS FUNCTIONS OF INITIAL PROPELLANT FUEL FRACTION

Fuel fraction	Molecular weight	Tem-pera-ture, $^{\circ}$K	Charac-teristic exhaust velocity, c^*, ft/sec	Fuel fraction	Molecular weight	Tem-pera-ture, $^{\circ}$K	Charac-teristic exhaust velocity, c^*, ft/sec
Oxygen-ammonia				Oxygen-hydrazine			
0.000000	32.000	298	1300	0.0	32	298	1300
.002	31.914	339	1426	.002	31.936	338	1424
.004	31.828	378	1510	.004	31.873	377	1506
.006	31.743	417	1590	.006	31.810	415	1584
.008	31.658	455	1666	.008	31.747	453	1659
.010417	31.557	500	1752	.010417	31.671	497	1743
.010989	31.533	511	1772	.010989	31.653	508	1763
.011628	31.506	522	1794	.011628	31.633	519	1784
.012346	31.476	535	1818	.012346	31.611	532	1808
.013158	31.442	550	1844	.013158	31.586	547	1834
.014085	31.404	567	1874	.014085	31.557	563	1864
.015152	31.539	586	1908	.015152	31.524	582	1897
.016393	31.308	608	1947	.016393	31.485	604	1935
.017857	31.248	633	1991	.017857	31.440	629	1979
.019608	31.176	663	2043	.019608	31.386	659	2029
.021739	31.089	699	2103	.021739	31.321	695	2089
.024390	30.981	743	2175	.024390	31.240	740	2160
.027778	30.845	798	2263	.027778	31.138	795	2247
.032258	30.666	869	2373	.032258	31.003	866	2355
.038462	30.422	964	2515	.038462	30.818	963	2495
.047619	30.069	1099	2707	.047619	30.550	1100	2686
.0625	29.513	1303	2987	.062500	30.123	1311	2962
.090909	28.504	1650	3442	.090909	29.339	1675	3415
.1000	28.194	1749	3571	.100000	29.095	1782	3543
.111111	27.823	1863	3720	.111111	28.800	1905	3692
.125	27.368	1996	3895	.125000	28.435	2048	3866
.142857	26.796	2149	4101	.142857	27.996	2215	4072
.166667	26.052	2327	4351	.166667	27.340	2408	4320
.2	25.041	2530	4659	.200000	26.457	2630	4622
.25	23.595	2763	5050	.250000	25.138	2880	4999
.333333	21.384	3023	5585	.333333	23.038	3163	5504
.357143	20.788	3074	5718	.350000	22.638	3205	5593
.384615	20.106	3116	5861	.400000	21.476	3312	5845
.416667	19.290	3130	6000	.450000	20.359	3384	6073
.454545	18.244	3057	6071	.500000	19.268	3413	6271
.50	16.893	2817	5980	.555556	18.067	3378	6430
.555556	15.310	2399	5721	.625000	16.596	3216	6495
.625	13.626	1850	5264	.650000	16.084	3128	6480
.65	13.103	1659	5065	.714286	14.832	2852	6368
.714286	11.932	1190	4447	.750000	14.183	2675	6267
.75	11.398	945	4039	.833333	12.813	2235	5952
.833333	11.981	605	3299	.850000	12.564	2146	5878
.90	13.489	510	2848	.905	11.805	1859	5610
.905	13.657	503	2813	.91	11.740	1833	5584
.91	13.830	497	2778	.915	11.677	1808	5558
.915	14.006	490	2743	.92	11.613	1783	5531
.92	14.187	483	2707	.925	11.551	1757	5504
.925	14.371	476	2671	.93	11.489	1732	5476
.93	14.559	469	2634	.935	11.427	1707	5448
.935	14.751	462	2597	.94	11.367	1682	5420
.94	14.945	454	2559	.945	11.307	1658	5391
.945	15.142	446	2519	.950000	11.248	1633	5363
.95	15.340	438	2479	.955	11.189	1608	5333
.955	15.540	429	2436	.96	11.131	1584	5304
.96	15.738	419	2392	.965	11.074	1560	5274
.965	15.935	409	2346	.97	11.017	1535	5244
.97	16.127	397	2297	.975	10.961	1511	5213
.975	16.313	385	2244	.98	10.905	1487	5182
.98	16.487	371	2186	.985	10.850	1463	5150
.985	16.644	355	2122	.99	10.796	1440	5119
.99	16.777	337	2049	.995000	10.742	1416	5087
.995	16.879	316	1965	1.00	10.699	1397	5061
.999	16.932	300	1889				
1.0	17.032	298	1834				

TABLE I. - Continued. EQUILIBRIUM MOLECULAR WEIGHT, TEMPERATURE, AND CHARACTERISTIC EXHAUST VELOCITY AS FUNCTIONS OF INITIAL PROPELLANT FUEL FRACTION

Fuel fraction	Molecular weight	Temperature, °K	Characteristic exhaust velocity, c^*, ft/sec
	Oxygen - JP-4		
0.0	32	298	1300
.006	31.978	572	1868
.008	31.971	658	2010
.010417	31.963	758	2165
.010989	31.961	781	2200
.011628	31.958	807	2237
.012346	31.956	835	2279
.013158	31.953	867	2324
.014085	31.949	904	2375
.015152	31.946	945	2432
.016393	31.941	993	2495
.017857	31.936	1049	2567
.019608	31.930	1114	2650
.021739	31.922	1193	2745
.024390	31.913	1289	2859
.027778	31.900	1409	2995
.032258	31.884	1563	3162
.038462	31.859	1767	3375
.047619	31.812	2049	3654
.0625	31.654	2441	4039
.090909	30.881	2928	4558
.1	30.527	3028	4676
.111111	30.057	3128	4802
.125	29.436	3228	4938
.142857	28.615	3327	5091
.166667	27.518	3424	5271
.2	26.026	3515	5493
.25	23.909	3575	5774
.263158	23.369	3574	5837
.277778	22.774	3562	5898
.294118	22.108	3533	5953
.312500	21.349	3472	5989
.333333	20.471	3360	5986
.357143	19.451	3169	5916
.384615	18.283	2880	5753
.416667	16.981	2479	5470
.454545	15.592	1968	5029
.500000	15.307	1668	4710
.555556	15.537	1471	4458
.625	16.227	1324	4198
.65	16.565	1286	4110
.714286	17.615	1208	3887
.75	18.309	1169	3759
.833333	20.288	1077	3441
.850000	20.754	1057	3372
.90	22.319	991	3151
.905	22.489	984	3128
.91	22.662	976	3104
.915	22.873	969	3081
.92	23.015	961	3057
.925	23.195	953	3033
.93	23.377	945	3009
.935	23.562	937	2984
.94	23.748	929	2960
.945	23.936	920	2935
.95	24.126	912	2910
.955	24.317	903	2885
.96	24.509	894	2859
.965	24.702	885	2834
.97	24.896	875	2808
.975	25.090	866	2782
.98	25.284	856	2756
.985	25.478	846	2729
.99	25.671	836	2703
.995	25.863	825	2676
1.0	26.014	816	2654

Fuel fraction	Molecular weight	Temperature, °K	Characteristic exhaust velocity, c^*, ft/sec
	Fluorine-hydrogen		
0.0	38.0	298	1240
.002	36.606	863	2187
.004	33.896	1177	2727
.006	30.704	1334	3063
.008	27.872	1444	3342
.010417	25.030	1558	3651
.010989	24.443	1584	3721
.011628	23.823	1614	3800
.012346	23.170	1648	3888
.013158	22.485	1690	3987
.014085	21.773	1742	4101
.015152	21.046	1813	4234
.016393	20.344	1919	4394
.017857	19.769	2103	4596
.019608	19.489	2437	4878
.021739	19.447	2916	5306
.024390	19.477	3497	5838
.027778	19.438	4090	6451
.032258	19.041	4451	7044
.038462	18.261	4620	7417
.047619	17.085	4667	7733
.062500	15.385	4555	8041
.090909	12.973	4136	8291
.100000	12.380	4010	8350
.111111	11.732	3869	8420
.125000	11.014	3711	8502
.142857	10.204	3526	8594
.147059	10.029	3484	8613
.151515	9.849	3441	8632
.156250	9.664	3396	8650
.161290	9.474	3348	8667
.166667	9.278	3298	8684
.172414	9.076	3246	8699
.178571	8.867	3190	8712
.185185	8.652	3130	8723
.192308	8.430	3067	8731
.200000	8.201	2999	8735
.208333	7.964	2926	8735
.217391	7.719	2847	8729
.227273	7.466	2762	8718
.238095	7.204	2670	8700
.250000	6.935	2572	8676
.333333	5.467	1971	8449
.350000	5.243	1872	8396
.400000	4.668	1612	8227
.450000	4.207	1397	8042
.500000	3.829	1216	7842
.550000	3.513	1062	7631
.600000	3.245	928	7411
.650000	3.015	812	7183
.700000	2.816	710	6948
.750000	2.641	621	6705
.800000	2.487	542	6452
.850000	2.350	471	6189
.900000	2.227	408	5913
.905	2.215	402	5885
.91	2.204	396	5856
.915	2.192	390	5828
.920000	2.181	384	5799
.925	2.170	379	5770
.93	2.159	373	5740
.935	2.148	367	5711
.94	2.137	362	5682
.945	2.127	356	5652
.950000	2.116	351	5622
.955	2.106	346	5592
.96	2.095	340	5562
.965	2.085	335	5531
.97	2.075	330	5501
.975	2.065	325	5470
.98	2.055	319	5439
.985	2.045	314	5408
.99	2.035	309	5377
.995	2.026	304	5345
.999	2.018	300	5319
1.0000	2.016	298	5311

TABLE I. - Continued. EQUILIBRIUM MOLECULAR WEIGHT, TEMPERATURE, AND CHARACTERISTIC EXHAUST VELOCITY AS FUNCTIONS OF INITIAL PROPELLANT FUEL FRACTION

Fuel fraction	Molecular weight	Temperature, °K	Characteristic exhaust velocity, C*, ft/sec	Fuel fraction	Molecular weight	Temperature, °K	Characteristic exhaust velocity, C*, ft/sec
Fluorine-ammonia				Fluorine-hydrazine			
0.0	38	298	1240	0.0	38	298	1240
.002	37.907	421	1478	.002	37.986	403	1445
.004	37.814	536	1679	.004	37.972	503	1622
.006	37.719	646	1853	.006	37.957	599	1776
.008	37.613	752	2008	.008	37.938	692	1915
.010989	37.366	894	2214	.010417	37.892	798	2067
.011628	37.289	921	2255	.010989	37.873	822	2101
.012346	37.191	950	2299	.011628	37.847	848	2138
.013158	37.063	981	2346	.012346	37.810	876	2178
.014085	36.894	1012	2397	.013158	37.758	907	2222
.015152	36.667	1045	2452	.014085	37.683	940	2271
.016393	36.357	1078	2511	.015152	37.574	975	2324
.017857	35.934	1110	2572	.016393	37.415	1011	2382
.019608	35.377	1141	2636	.017857	37.173	1049	2444
.021739	34.673	1175	2705	.019608	36.806	1085	2511
.024390	33.804	1211	2783	.021739	36.271	1121	2580
.027778	32.738	1253	2877	.024390	35.546	1156	2652
.032258	31.417	1304	2995	.027778	34.609	1196	2734
.038462	29.742	1366	3150	.032258	33.420	1242	2836
.047619	27.556	1448	3364	.038462	31.894	1300	2969
.062500	24.624	1570	3691	.062500	27.056	1480	3431
.090909	20.836	1886	4311	.047619	29.869	1374	3153
.1	20.242	2098	4534	.090909	23.002	1676	3927
.111111	20.052	2497	4872	.100000	22.023	1753	4086
.125	20.122	3056	5378	.111111	21.053	1880	4287
.142857	20.263	3718	5975	.125000	20.332	2150	4564
.166667	20.158	4242	6636	.142857	20.212	2707	5034
.2	19.524	4440	7036	.166667	20.384	3486	5724
.208333	19.337	4450	7087	.200000	20.420	4245	6541
.217391	19.129	4450	7132	.250000	19.716	4542	7079
.227273	18.899	4439	7169	.263158	19.486	4560	7145
.238095	18.646	4416	7198	.277778	19.224	4565	7204
.25	18.367	4378	7215	.294118	18.928	4555	7255
.263158	18.063	4321	7217	.312500	18.594	4528	7295
.277778	17.733	4242	7202	.333333	18.220	4477	7321
.294118	17.380	4141	7169	.357143	17.804	4397	7325
.3125	17.006	4017	7123	.384615	17.347	4282	7303
.333333	16.610	3875	7065	.416667	16.856	4133	7261
.357143	16.186	3713	6995	.454545	16.331	3955	7204
.384615	15.721	3529	6903	.500000	15.758	3750	7131
.416667	15.196	3313	6777	.555556	15.107	3510	7028
.454545	14.585	3047	6591	.625000	14.332	3208	6859
.5	13.857	2703	6308	.714286	13.363	2789	6547
.555556	12.991	2257	5897	.750000	12.982	2610	6394
.625	12.012	1715	5308	.833333	12.133	2182	5998
.714286	10.959	1086	4384	.850000	11.972	2098	5913
.75	10.653	862	3979	.900000	11.511	1851	5647
.833333	11.446	595	3309	.905	11.467	1827	5620
.85	11.841	571	3196	.91	11.423	1803	5592
.9	13.330	508	2858	.915	11.380	1779	5564
.905	13.504	501	2824	.92	11.336	1755	5536
.91	13.681	495	2788	.925	11.293	1732	5507
.915	13.864	489	2753	.93	11.251	1708	5479
.92	14.050	482	2717	.935	11.209	1685	5450
.925	14.240	475	2680	.94	11.167	1662	5421
.93	14.435	468	2643	.945	11.125	1639	5392
.935	14.632	461	2605	.950000	11.084	1616	5362
.94	14.834	453	2566	.955	11.043	1593	5333
.945	15.037	445	2526	.96	11.002	1570	5303
.95	15.243	437	2485	.965	10.962	1548	5272
.955	15.451	428	2442	.97	10.922	1525	5242
.96	15.658	419	2398	.975	10.882	1503	5211
.965	15.863	408	2351	.98	10.843	1480	5180
.97	16.065	397	2301	.985	10.804	1458	5149
.975	16.260	385	2248	.99	10.765	1436	5118
.98	16.444	371	2189	.995	10.727	1414	5086
.985	16.612	355	2124	1.0	10.696	1397	5060
.99	16.756	337	2051				
.995	16.868	316	1966				
.999	16.930	300	1889				
1.0	17.032	298	1834				

TABLE I. - Concluded. EQUILIBRIUM MOLECULAR WEIGHT, TEMPERATURE, AND CHARACTERISTIC EXHAUST VELOCITY AS FUNCTIONS OF INITIAL PROPELLANT FUEL FRACTION

Nitrogen tetroxide - hydrazine

Fuel fraction	Molecular weight	Temperature, °K	Characteristic exhaust velocity, C*, ft/sec
0.0	30.670	424	1650
.002	30.616	461	1702
.004	30.560	497	1771
.006	30.505	532	1837
.008	30.449	567	1900
.010417	30.383	609	1973
.010989	30.367	619	1990
.011628	30.349	629	2009
.012346	30.330	642	2030
.013158	30.307	655	2053
.014085	30.282	671	2079
.015152	30.253	688	2108
.016393	30.219	709	2142
.017857	30.179	733	2181
.019608	30.132	761	2226
.021739	30.074	795	2280
.024390	30.003	837	2345
.027778	29.913	890	2424
.032258	29.794	958	2524
.038462	29.630	1050	2655
.047619	29.393	1180	2834
.0625	29.015	1381	3098
.090909	28.317	1728	3531
.100000	28.099	1829	3655
.111111	27.835	1946	3798
.125000	27.508	2083	3965
.142857	27.087	2243	4165
.166667	26.525	2432	4406
.200000	25.729	2652	4702
.250000	24.524	2906	5077
.263158	24.208	2961	5165
.277778	23.857	3017	5258
.294118	23.467	3073	5358
.312500	23.030	3130	5465
.333333	22.537	3185	5579
.357143	21.975	3236	5701
.384615	21.324	3278	5830
.416667	20.560	3300	5959
.454545	19.651	3285	6071
.500000	18.571	3209	6141
.555556	17.310	3052	6151
.625000	15.874	2799	6088
.714286	14.270	2441	5926
.750000	13.703	2297	5844
.833333	12.528	1971	5622
.850000	12.316	1909	5573
.900000	11.721	1728	5415
.905	11.664	1710	5399
.91	11.608	1693	5382
.915	11.553	1676	5365
.92	11.498	1658	5348
.925	11.444	1641	5331
.93	11.390	1624	5313
.935	11.337	1607	5296
.94	11.284	1590	5278
.945	11.232	1573	5260
.950000	11.180	1556	5242
.955	11.129	1539	5224
.96	11.078	1523	5206
.965	11.028	1506	5187
.97	10.978	1489	5169
.975	10.929	1473	5150
.98	10.880	1457	5131
.985	10.831	1441	5112
.99	10.783	1424	5093
.995	10.736	1408	5074
1.00	10.698	1396	5058

Oxygen-hydrogen

Fuel fraction	Molecular weight	Temperature, °K	Characteristic exhaust velocity, C*, ft/sec
0.0	32.000	298	1300
.002	31.562	546	1835
.004	31.136	770	2210
.006	30.721	975	2516
.008	30.318	1166	2781
.010417	29.844	1383	3062
.010989	29.733	1431	3124
.011628	29.612	1485	3194
.012346	29.476	1544	3265
.013158	29.323	1609	3345
.014085	29.151	1681	3433
.015152	28.956	1762	3532
.016396	28.731	1852	3641
.017857	28.469	1953	3764
.019608	28.160	2067	3904
.021739	27.789	2195	4064
.024390	27.732	2337	4249
.027778	26.751	2494	4462
.032258	25.984	2665	4712
.038462	24.931	2848	5008
.047619	23.430	3043	5374
.062500	21.210	3250	5867
.066667	20.642	3293	5991
.071429	20.020	3335	6127
.076923	19.337	3376	6277
.083333	18.585	3416	6445
.090909	17.750	3453	6634
.111111	15.772	3499	7089
.142857	13.225	3438	7653
.200000	9.946	3073	8216
.208333	9.578	3008	8261
.217391	9.203	2937	8300
.227273	8.823	2858	8335
.238095	8.437	2771	8363
.250000	8.046	2676	8384
.263158	7.651	2573	8397
.277778	7.252	2460	8402
.294118	6.852	2340	8398
.312500	6.450	2211	8384
.333333	6.048	2074	8358
.350000	5.760	1972	8332
.400000	5.040	1700	8222
.450000	4.480	1474	8077
.500000	4.032	1282	7903
.550000	3.565	1117	7705
.600000	3.360	974	7491
.650000	3.102	849	7263
.700000	2.880	739	7023
.750000	2.688	643	6773
.800000	2.520	558	6511
.850000	2.372	482	6237
.900000	2.240	415	5947
.905	2.228	408	5918
.910000	2.215	402	5887
.915000	2.203	396	5857
.92	2.191	390	5827
.925	2.179	384	5796
.93	2.168	378	5765
.935	2.156	372	5734
.94	2.145	366	5703
.945	2.133	360	5672
.950000	2.122	354	5640
.955	2.111	348	5609
.96	2.100	343	5577
.965	2.089	337	5544
.97	2.078	332	5512
.975	2.068	271	5479
.98	2.057	321	5447
.985	2.047	315	5413
.990000	2.036	310	5380
.995	2.026	305	5347
.999	2.018	300	5320
1.00	2.016	298	5311

NASA-Langley, 1965 E-2842